Metals & corrosion

Investigating defect evolution during thermal treatment in Ni–Cr alloy using positron annihilation spectroscopy

Priya Maheshwari[1,2,*] , N. Keskar[3], K. Sudarshan[1,2], K. V. Manikrishna[3], Madangopal Krishnan[3,4], and
P. K. Pujari[1,2,*]

[1] Radiochemistry Division, Bhabha Atomic Research Centre, Mumbai, India
[2] Homi Bhabha National Institute, Anushaktinagar, Mumbai, India
[3] Mechanical Metallurgy Division, Bhabha Atomic Research Centre, Mumbai, India
[4] Materials Group, Bhabha Atomic Research Centre, Mumbai, India

ABSTRACT

Defects evolved during thermal treatment in high Cr content Ni–Cr alloy have been studied using Positron lifetime and coincidence Doppler broadening spectroscopy complemented with microscopic technique. The single-phase gamma-quenched specimen obtained by solutionization at 1200 °C has been thermally aged at 650 °C and 800 °C. Thermal treatment resulted in the phase transformation of the matrix through precipitation of Cr. It is seen that solutionization treatment followed by quenching resulted in the stabilization of thermal vacancies generated at 1200 °C which effectively trap the positrons. The results infer that these vacancies may form vacancy-Cr complexes which act as nucleation site for Cr aggregation. Positron lifetime and momentum distribution of annihilation electrons indicated that in the aged alloys, positrons are trapped in vacancy-like defects (vacancy clusters/vacancy-solute complex) and the interface between Cr precipitate and matrix, the latter becoming more predominant with subsequent ageing. At the highest ageing studied, vacancy-like defects are evolved within the Cr precipitates. The results indicated that positron trapping sites (vacancies and precipitate interface) are not specific to either Ni or Cr atoms which surround the trapping site in nearly equal proportion. Therefore, unambiguous identification of the defect type at each stage of thermal treatment becomes difficult. Considering positron trapping at the surface of precipitates, we have calculated positron specific trapping coefficient to be $\sim 1.33 \times 10^{-6}$ cm^3 s^{-1}, which is of the order estimated for large voids and estimated the number density of precipitates.

Introduction

The solid-state reactions involving phase transformation of a single-phase matrix to a two-phase system are important for improving the properties of alloys. The mechanical performance of many advanced structural materials is mainly derived from the presence of a hardening second phase [1]. Age hardening controlled by precipitation reactions [2–4] and nanoparticles [5] is amongst the various strengthening mechanisms used to improve the mechanical properties of engineering alloys. It provides mechanical strength, wear, creep, corrosion and fatigue resistance to the alloy. The synergistic effect of composition and microstructure of the hardening phase can be utilized for improving the mechanical properties of the material. Precipitation is one of the solid-state reactions transforming the initial phase composition to a two-phase system of matrix and precipitates [6]. The precipitate phase may differ in crystal structure, composition and degree of long-range order from the initial parent phase as well as the resultant product matrix [7]. In general, precipitation takes place through formation, migration, mutual recombination and annihilation of point defects like vacancies and interstitials. The role of quenched-in vacancies, vacancy-solute complex and solute clusters during precipitation reaction has been investigated for a number of alloys [8–10]. These defects mediate the course of transformation reaction as well as influence the resultant properties of the transformed alloy [11]. Therefore, investigation of defects evolved during phase transformations is essential to understand not only the mechanism of transformation but devise better preparation methodology of new alloys with desired properties.

Ni-based alloys have attracted wide attention due to their excellent mechanical strength, resistance to thermal creep and oxidation. These alloys are strengthened mainly by ordered and coherent intermetallic precipitates [12–14]. Precipitation-hardened Ni alloys have applications in high-temperature components of gas turbine and steam generators [15, 16]. Cr addition imparts high oxidative resistance to these alloys. However, the solubility of Cr in Ni decreases with the decrease in temperature, leading to precipitation of α-Cr in the two-phase region of Ni–Cr phase diagram [12, 17]. Depending on Cr content and thermal treatment, Cr precipitates of various morphologies such as discontinuous (cellular) and continuous have been reported in high Cr content Ni-based alloys [6, 18]. The discontinuous precipitation (DP) involves heterogeneous precipitation along the grain boundary with concurrent growth of the precipitate being mediated by the migration of the grain boundary, whilst continuous precipitation involves the uniform appearance of precipitates throughout the matrix [7, 19]. The precipitation behaviour influences the properties of alloy in different ways. In the present study, we have investigated the evolution of defects during thermal treatment in high Cr content Ni–Cr alloy using positron annihilation spectroscopy (PAS) complemented with microscopic technique. Microscopic techniques like Scanning Electron Microscopy (SEM) and Transmission Electron Microscopy (TEM) are well-established and sensitive techniques to probe microstructural transformations with as fine a resolution ~ 1 nm. However, the microscopic investigation is, by nature, limited to a localized region and may not represent the bulk microstructure. On the other hand, PAS is a powerful technique for the identification of atomic order defects and, can provide information with just as fine a resolution as TEM, but over a much larger volume. The sensitivity of positrons to low-electron density regions enables the identification of defects (vacancy, dislocation, lattice misfits, etc.) in alloys. The ability of the technique for the investigation of embedded nanoclusters [20, 21], Cu precipitates in Fe–Cu alloys [22, 23], age hardening in Al-Sn alloys [24] and fine grain materials [25] is well documented. These studies have shown the potential of the technique to investigate subtle structural transformations during decomposition reactions in solid-solutions.

When a positron is implanted in a material, it gets thermalized and then diffuses into the matrix. The low-electron density regions like open-volume defects and vacancies act as an attractive potential for positron and trap the positron. In a defect-free material, positron can diffuse to a longer distance (up to a few 100 of nm) and annihilates from a delocalized state with a characteristics bulk lifetime. On the other hand, annihilation from the trapped state is manifested as an increase in positron lifetime compared to the bulk lifetime. The self-seeking ability of positron for defects enables the identification of defects in concentration as low as a few ppm. The size of the defect is manifested in positron lifetime,

whilst chemical surrounding of the defect can be obtained from the annihilation electron momentum distribution using positron lifetime and coincidence Doppler broadening spectroscopy, respectively. Therefore, PAS can provide information about vacancy, vacancy-solute complexes and open-volume defects which are generally formed during precipitation reactions in the alloys.

In the present paper, we demonstrate the sensitivity of the positron technique towards the identification of defects evolved during thermal treatment in Ni–Cr alloy. The positrons are primarily trapped in quenched-in vacancies and the interface of Cr precipitate and the matrix during thermal treatment. The results suggest that trapping at the precipitate interface increases with ageing, and with subsequent ageing vacancy-like defects are evolved within the Cr precipitates. The momentum distribution of annihilation electrons at the trapping sites indicates that defects are not specific to Ni and Cr which surround the trapping site in nearly equal fractions except for vacancy-like defects. Therefore, we could not estimate the fraction of annihilation from quenched-in vacancies and interfaces at each stage of the precipitation. We have estimated positron-specific trapping coefficient for the interfaces under the assumption of positron trapping at the surface of precipitates and approximated the number density of precipitates.

Materials and methods

A cold-rolled (70% reduction) sample of Ni–Cr alloy (42 wt% Cr or, 44.6 at%Cr) is solutionized at 1200 °C, followed by water quenching, to attain a single-phase (namely, γ-phase) gamma-quenched (GQ) microstructure. The single-phase microstructure sample is referred as gamma-quenched (GQ) throughout the manuscript. Different specimens of size ∼ 15 × 15 mm are prepared from the GQ sample and subjected to ageing at 650 °C and 800 °C for different time periods (0.25–24 h). In order to freeze the microstructure following the thermal treatment, the samples are water quenched. For microstructural observations, the surfaces of the heat-treated samples are subjected to metallographic polishing and etching. For polishing, first, the samples are mounted in Condufast ® conducting mounting resin using a Struers ® CitoPress mounting press. These mounted samples of 25 mm diameter are then polished using

progressively finer grades of SiC polishing papers (FEPA P# 500 to FEPA P# 2400) using water for cooling and lubrication. This is followed by fine polishing using diamond suspensions with particle sizes of 3 and 1 μm. A final polishing has been carried out using colloidal silica suspension with a particle size of ∼ 40 nm. The samples are then subjected to electro-etching with a saturated (10% by weight) solution of chromic acid at 6 V for 10–15 s. After thorough cleaning and drying, the samples are investigated using a Carl Zeiss Auriga Cross Beam®Field Emission Gun Scanning Electron Microscope (FESEM).

Positron lifetime (PL) measurements are carried out using fast–fast coincidence system employing two BaF_2 detectors in a 90° configuration with respect to each other. The ^{22}Na positron source with an activity of ∼ 20 μCi and sealed in ∼ 8 μm polyimide film is used for PL measurements. The source is sandwiched between two identical specimens of the sample. The time resolution of the spectrometer is 245 ps. The source contribution arising from positron annihilation in positron source and encapsulating foil is obtained using Si wafer as reference and corrected for the difference in back-scattering fraction in Ni-based samples. PL measurements are performed at room temperature and spectrum with at least 2×10^6 counts is acquired for each measurement. The PL spectra are analysed using PALSfit [26]. All the spectra could be fitted with two lifetime components with $\lambda^2 \leq 1.02$.

Coincidence Doppler broadening (CDB) measurements are carried out using two high purity Germanium (HPGe) detectors with an energy resolution of ∼ 1.2 at 514 keV, located at 180° relative to each other at a distance of ∼ 8 cm apart. The coincident count rate is ∼ 400 per s for 20 μCi ^{22}Na positron source (similar to that used in lifetime measurements) and at least 10^7 counts are recorded for each Doppler broadening spectrum. The annihilation electron momentum distribution is obtained by selecting the coincidence events where the sum of annihilation γ-ray energies detected is in the range $2m_oc^2 \pm 2.4$ keV, where m_oc^2 is electron rest mass energy. The details of the analysis are reported elsewhere [27]. The annihilation electron momentum distribution of annealed Ni and Cr is also measured to compare the momentum distribution of all the samples. The shape of the annihilation electron momentum distribution curve, represented as the

ratio with respect to the momentum distribution of a reference, exhibits information about elemental profiles at the annihilation site.

Results and discussion

Microstructure evolution

The microstructure of the Ni 42 wt% Cr alloy during thermal ageing indicates that precipitation is initiated at grain boundaries and subsequently, colonies of precipitates (namely, discontinuous precipitation (DP) cell) grow towards the interior of the grains. Figure 1 represents the microstructure of the matrix after thermal ageing at 650 °C for 24 h and 800 °C for 6 h indicating the extent of matrix transformation at the two temperatures. At 650 °C, precipitates localized primarily near the grain boundaries are seen at 24 h ageing, whilst colonies of precipitates occupying a larger volume of the grain are observed even at 6 h of ageing at 800 °C. The average grain size of the single-phase GQ is about 100–200 μm, which remains invariant during the studied ageing treatment. The evolution of microstructure with thermal ageing at 650 °C and 800 °C is shown in Figs. 2 and 3, respectively, indicating slower precipitation kinetics at 650 °C than 800 °C. At 650 °C, though precipitation is initiated at 1 h ageing, precipitates are mainly localized near the grain boundary region even after 24 h of ageing and could be identified at higher magnifications. On the other hand, at 800 °C, within 4 h of ageing, precipitates occupy a large fraction of the grain volume. The growth behaviour of precipitates shows that DP is the dominant microstructural feature at these temperatures similar to that reported in an earlier publication from this laboratory [18]. The precipitation reaction is initiated at the grain boundaries and subsequently, precipitates grow towards the interior of the grains occupying a large fraction of the grain volume. The microstructural analyses show that at 800 °C, after 1 h ageing ∼ 8% of the phase transformation has taken place, which increases to ∼ 100% at 24 h ageing. In the same time duration (1–24 h), at 650 °C ageing, the transformed fraction has a modest increase from ∼ 3 to ∼ 8%. The transformed phase fraction in a micrograph is calculated by manually identifying the total area occupied by the DP cells in that micrograph and dividing it by the total area of the micrograph. The average area fraction calculated over a number of micrographs from different areas of the same sample is considered. The result indicates that complete phase transformation is achieved at 24 h ageing at 800 °C and no more Cr can precipitate out from the matrix. The fraction of phase transformation estimated from microscopic measurements is shown in Table 1.

Figure 4a is a representative image (sample aged for 6 h at 800 °C) indicating lamellar-like morphology of the precipitates and different DP cells with a specific orientation of precipitates occupying a significant fraction of the grain volume. The energy dispersive X-ray (EDX) mapping of a section of DP cell (Fig. 4b) shows that Cr precipitates (seen as Cr enrichment in the EDX map) are present only within the DP cell, in conjunction with corresponding local Ni enrichment in the interlamellar region. The microstructure indicates that a DP cell comprises alternate regions of Ni and Cr enrichment. There is no Cr enrichment in the surrounding untransformed matrix, indicating that Cr precipitates are not homogeneously distributed in the matrix. The detailed analyses of chemical composition and orientation relationship of the precipitate phase using

Figure 1 SEM micrographs of the microstructure of Ni–Cr alloy aged for **a** 24 h at 650 °C and, **b** 6 h at 800 °C, representing extent of matrix transformation during thermal ageing at 650 °C and 800 °C.
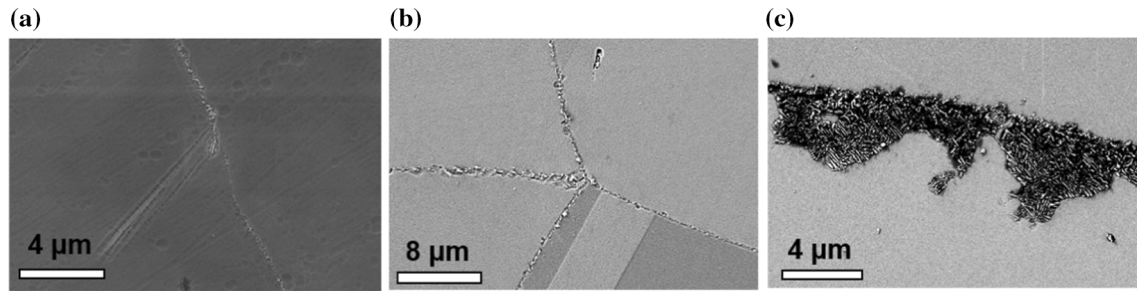

(a) 650°C, 24 h 50 μm

(b) 800°C, 6 h 50 μm

(a) **(b)** **(c)**
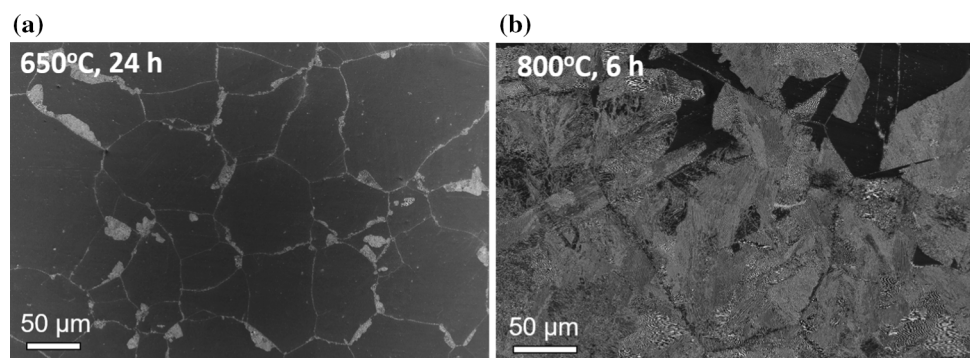
Figure 2 SEM micrographs representing the evolution of precipitates for Ni–Cr alloy aged at 650 °C for **a** 1 h **b** 6 h **c** 24 h.
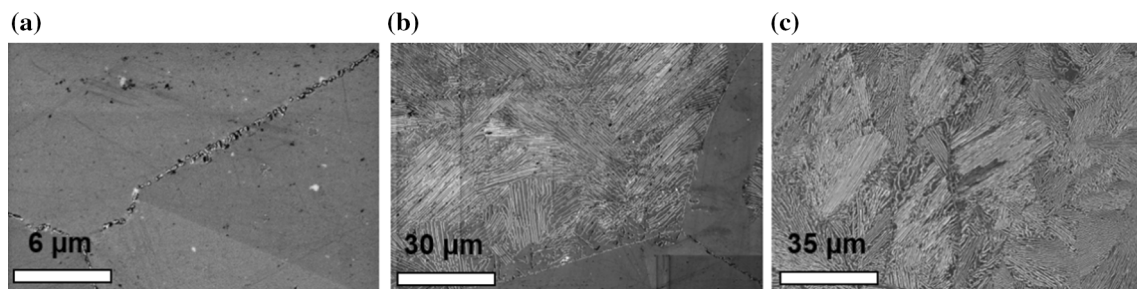
(a) **(b)** **(c)**

Figure 3 SEM micrographs representing the evolution of precipitates for Ni–Cr alloy aged at 800 °C for **a** 15 min **b** 4 h and **c** 24 h.

Table 1 The fraction of phase transformation obtained from microscopic analysis during ageing at 650 °C and 800 °C indicating volume fraction of Cr segregated from the matrix

Ageing time (h)	Phase transformation (%) T = 650 °C	Phase transformation (%) T = 800 °C
1	3	8
4	3	48
6	5	61
24	8	100

(a)

(b)

No Cr enrichment in matrix
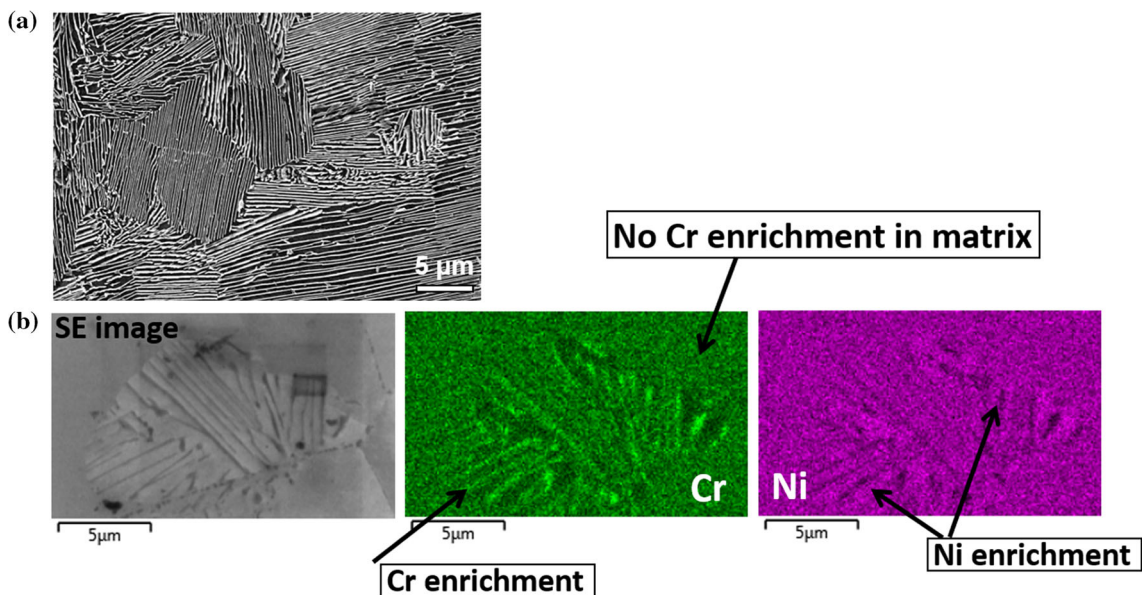
SE image

Cr Ni

Cr enrichment

Ni enrichment

Figure 4 **a** Image representing the lamellar morphology of the precipitates. **b** Energy dispersive X-ray (EDX) map of a section of a DP cell showing elemental distribution of Ni and Cr.

transmission electron microscopy have been reported in a previous publication [18].

Positron annihilation measurements

Positron lifetimes obtained from the decomposition of a PL spectrum represent different positron annihilation sites/positron states in a material. The measured positron lifetimes in well-annealed Ni and Cr are 104 and 115 ps, respectively, which are in good agreement with the previous reports [28]. The positron lifetimes in GQ and 70% cold-rolled alloy have also been measured and shown in Table 2. The cold-rolled sample shows a single positron lifetime ca. $\tau \sim 168$ ps which corresponds to dislocations in Ni-based alloys [28]. In contrast, the single-phase GQ sample, shows two positron lifetime components viz. $\tau_1 \sim 106$ ps and $\tau_2 = 243$ ps with corresponding intensities 86.04 and 13.88%, respectively. The longer lifetime (τ_2) is seen to be in the range of positron lifetimes in large vacancy clusters in Ni-based alloys. The reported positron lifetimes in various kinds of defects in Ni (very few are available for Cr) are shown in Table 3 [29, 30]. The decomposition of the lifetime spectrum into two distinct lifetimes indicates the presence of point defects in the GQ phase. The measured mean positron lifetime in the GQ phase is $\tau_{avg} = 125$ ps which is higher than that in a defect-free Ni or Cr. Therefore, we attribute the shorter positron lifetime component (τ_1) to free positron annihilation and the second component (τ_2) to be from positrons trapped at defects. The bulk positron lifetime in the defect-free GQ phase will be different than that of pure defect-free Ni or Cr and can be obtained under the consideration of the standard trapping model (STM). According to STM, in case of positron trapping in a defect, the free positron lifetime gets reduced from the bulk value and the second component represents positron lifetime in the defect [31, 32]. Consequently, the annihilation rates for the two positron states are expressed as follows:

$$\lambda_1 = \lambda_b + k_d \tag{1}$$

$$\lambda_2 = \lambda_d \tag{2}$$

where λ_1, λ_b, λ_d represent the reduced-bulk, bulk and trapped positron annihilation rates, respectively, and k_d is the positron trapping rate in the defect, defined as: $k_d = \mu_d C$, where μ_d is the positron specific trapping coefficient that depends on the type of the defect and C is the defect concentration. Subsequently, the positron lifetime in the bulk is given by

$$\tau_b = \frac{\tau_1 \tau_2}{\tau_1 I_2 + \tau_2 I_1} \tag{3}$$

Using Eq. 3, the positron lifetime in the bulk GQ phase is estimated to be ~ 115 ps. The GQ sample is prepared by high-temperature solutionization treatment followed by water quenching to obtain the single-phase microstructure. During the heat treatment, thermal vacancies generated at a particular temperature can be retained in the matrix due to their incomplete recovery during quenching and/or presence of solute atoms which can stabilize vacancies by forming vacancy-solute complexes. The equilibrium atomic concentration of thermal vacancies formed at 1200 °C in Ni–Cr alloy is $\sim 3.93 \times 10^{-7}$ assuming the reported value of vacancy formation energy in Ni as ~ 1.77 eV [33]. Considering the presence of vacancy clusters (based on measured positron lifetime) and corresponding positron specific trapping coefficient ($\mu = i\mu_1$ where $\mu_1 = 1.5 \times 10^{14}$ s^{-1} is positron specific trapping coefficient for Ni monovacancy [31, 34] and i is the number of vacancies in the cluster), the trapped positron intensity (I_2) would be $\sim 7\%$. In addition, grain boundaries can also trap positrons. The contribution from open-volume defects present at the grain boundaries is less than 1%, considering the average grain size of 150 μm and positron diffusion length in single crystal defect-free Ni to be ~ 0.25 μm [30] (the maximum diffusion length that can be observed in a metal). Even when the positron diffusion length ~ 0.1 μm (typical for metals) is considered, the contribution from grain boundaries would be negligible. It may be noted that

Table 2 Positron lifetime in GQ and cold-rolled Ni–Cr alloy at room temperature

Sample	τ_1 (ps)	τ_2 (ps)	I_1 (%)	I_2 (%)
Gamma quenched (GQ)	106.2 ± 0.8	243.0 ± 5.7	86.04 ± 0.91	13.88 ± 0.91
70% Cold-roll	167.7 ± 0.3	–	$\sim 100\%$	–
96 h aged (at 650 °C)	106.0 ± 1.8	228.7 ± 7.8	80.83 ± 2.02	19.17 ± 2.02

Table 3 Positron lifetime in bulk and various types of defects in Ni as reported in the literature

Ref [28]		Ref [31]		Ref [30]	
Bulk	108 ps	V7 loop	200 ps	Strained (single crystal)	220 ps
Monovacancy	177/180 ps	V19 loop	293 ps	H_2 charged (single crystal)	219 ps
		SFT (V3–V28)	180–130 ps	Strained + H_2 charged (single crystal)	280 ps
				Strained (polycrystalline)	218 ps
				H_2 charged (polycrystalline)	255 ps
				Strained + H_2 charged (polycrystalline)	308 ps

The lifetime values are in ps

since positrons are randomly implanted in a material, this estimate is an approximate value.

Neglecting the small contribution from grain boundaries, we may attribute the second component to be from vacancy clusters. The alloy contains high Cr content with low solubility of Cr in Ni which reduces drastically with the decreasing temperature. Therefore, there is a fair possibility of stabilization of vacancies in the GQ sample due to the formation of the vacancy-Cr solute complex. It is well known that vacancies mediate the migration of solute atoms and thereby promote the segregation of solute atoms. We conjecture that the stabilization of vacancies in the GQ sample helps in promoting the Cr precipitation during subsequent thermal treatment. The presence of a significant number of vacancy defects (vacancy clusters and/or,vacancy-Cr complex) in the GQ phase, revealed from positron measurements is an important observation, as these defects in the GQ sample cannot be observed by microscopy technique.

PL spectra of alloys aged at 650 °C and 800 °C could be fitted to two lifetime components similar to the GQ sample with $\tau_1 \sim 103$–108 ps and $\tau_2 \sim 246$–210 ps (ageing from 0.25 to 24 h). The variation of mean positron lifetime (τ_{avg}) during ageing is shown in Fig. 5. The mean positron lifetime over the whole ageing period is seen to be greater than 125 ps which is higher than the bulk positron lifetime in the GQ phase (i.e. 115 ps). This signifies the presence of positron trapping sites (or, defects) in aged samples. Therefore, the second lifetime component is attributed to positron annihilation from trapped states in the alloy. As one can see, there is no significant change in mean positron lifetime on ageing at 650 °C over the whole ageing period whereas, on ageing at 800 °C, the mean lifetime shows an increase at 12 h and reaches to ~ 150 ps for 24 h
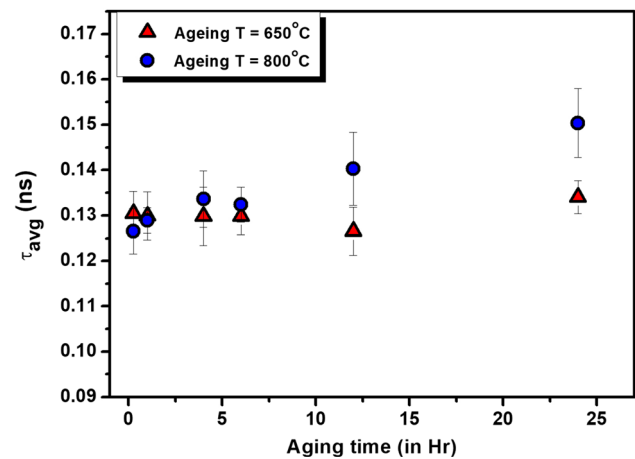
Figure 5 The average positron lifetimes (τ_{avg}) for Ni–Cr alloy aged at 650 °C and 800 °C.

ageing. The increase of mean lifetime indicates a significant increase in positron trapping for ageing periods longer than 12 h at 800 °C.

The variation of positron lifetimes (τ_1, τ_2) and trapped positron intensity (I_2) at different ageing time is shown in Fig. 6. At both the temperatures, τ_1 is nearly invariant during the ageing treatment whereas τ_2 and I_2 show significant change on ageing at 800 °C as compared to 650 °C. The change in τ_2 and I_2 is representative of the evolution of defects during the thermal ageing of the alloy. On ageing at 650 °C, there is only a marginal variation in τ_2 and I_2 over the entire ageing period. Therefore, it is difficult to access the evolution of defects from positron measurements in the samples aged at 650 °C. Due to slower precipitation kinetics as seen from microscopic measurements, the microstructural changes in the matrix are not substantial and, therefore, the positron data do not show significant variations for ageing at 650 °C. Even for 96 h ageing at this temperature, no significant change in τ_2 and I_2 (Table 2) is observed.
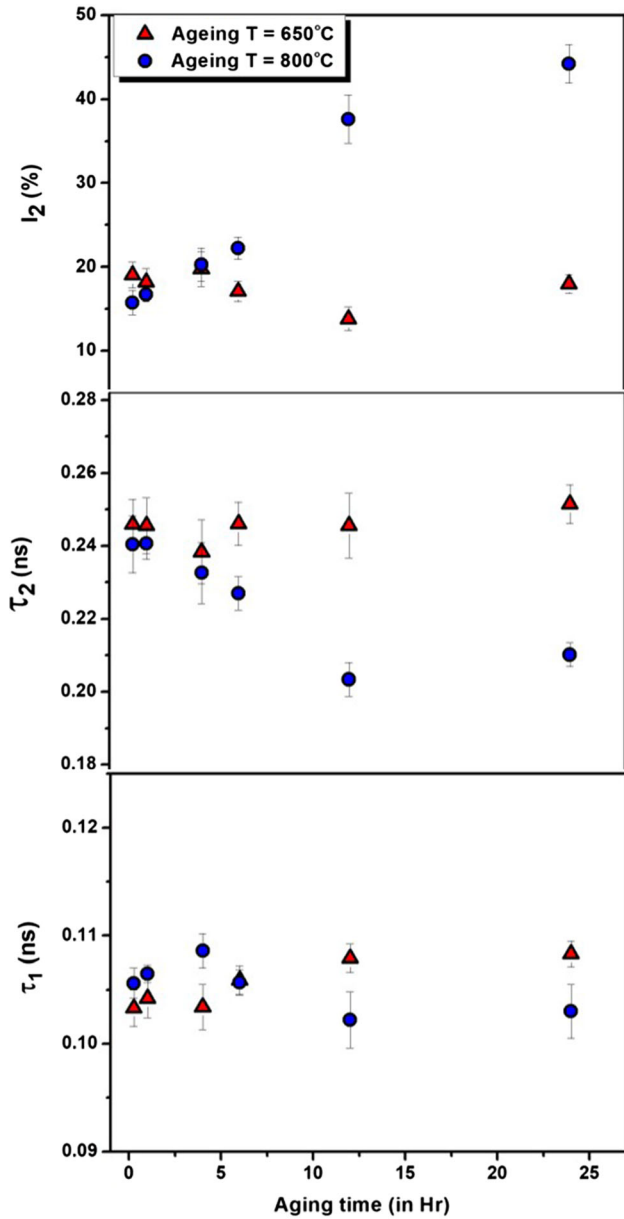
Figure 6 Positron lifetimes (τ_1 and τ_2) and intensity (I_2) for Ni–Cr aged at 650 °C and 800 °C for different ageing times. The solid line for 650 °C ageing treatment is an eye guide.

On the other hand, at 800 °C ageing, τ_2 is seen to decrease with the corresponding I_2 showing an increasing trend when aged from 15 min to 24 h. The τ_2 decreases from 240 to 210 ps and I_2 is seen to increase to 44% at the highest ageing. The I_2 increases by $\sim$ 22% during ageing from 15 min to 24 h. The positron trapping at thermal vacancies and grain boundaries, as seen in the GQ sample, cannot account for the increase in I_2 in aged samples. This is because the equilibrium atomic concentration of thermal

vacancies at 800 °C is lower than that at 1200 °C and, therefore, would not increase with thermal ageing treatment. For grain boundaries, the microscopic measurements have shown that there is no grain shrinkage or growth during thermal ageing at these temperatures. Hence, the contribution from grain boundaries will not be responsible for the observed increase in I_2. Therefore, we may infer that the change in I_2 manifests phase transformation of the matrix due to thermal ageing.

In this regard, it is worth mentioning that the solubility of Cr in Ni drops sharply with decreasing temperature and Cr can easily precipitate out from Ni–Cr alloy. For the present alloy, the microscopy measurements have shown precipitation of Cr on ageing at 650 °C and 800 °C. The matrix transformation due to precipitation is always associated with coevolution of defects and secondary phase. Positron trapping at defects as well as secondary phase (i.e. precipitates) can, therefore, manifest microstructural changes during the phase transformation. In the present alloy, Cr precipitates in the Ni matrix are not an efficient site for positron trapping due to lower positron affinity of Cr (-2.62 eV) than Ni (-4.46 eV) [35]. It is well known that positron trapping in a defect-free embedded precipitate/nanocluster is possible when the positron affinity of the precipitate is higher than the matrix [35, 36]. The positron trapping in Cr precipitates would be favoured only when precipitates are associated with defects. However, the interface between Cr precipitate and matrix can trap positrons due to the presence of open-volume defects at the interface. The presence of open-volume defects at the interface and positron trapping therein has also been observed by many researchers [22, 24, 31]. Therefore, we ascribe the change in τ_2 and I_2 to the coevolution of defects and Cr precipitates during thermally ageing.

It is well known that vacancies mediate migration of solute atoms in the alloys and subsequently solute separation. At the early stage of phase segregation, solute atoms form complex with the vacancies forming a vacancy-solute complex which acts as nucleation site for clustering of solute atoms. Subsequently, these clusters grow into precipitates under thermodynamic and kinetic constraints. At 800 °C, the initial increase in I_2 (up to 4 h) can be ascribed to the increase in the number of nucleation sites (or, vacancy-solute complex) with a concomitant decrease in its size as indicated from the decrease in τ_2. It is

interesting to note that τ_2 and I_2 at 800 °C and 650 °C for ageing up to 4 h are nearly similar. This clearly indicates a contribution from vacancy and/or, vacancy-solute complexes whose concentration would be nearly identical during the early stages of the thermal treatment at 650 °C and 800 °C as these vacancies are being stabilized during gamma-quenching treatment. The I_2 increases sharply beyond 4 h ageing at 800 °C unlike at 650 °C where there is no significant change in I_2. Most of the phenomenological models used to explain phase separation in solid solutions assume vacancies to be at equilibrium [37]. Therefore, the sharp increase in I_2 beyond 4 h cannot account for an increase in the number of vacancy-like defects. Henceforth, we envisage that the interface between precipitate and matrix is a potential positron trapping site for samples aged for longer durations (> 4 h) and responsible for a sharp increase in I_2. This is reasonable as precipitates occupy a large volume fraction of grains at these ageing times as revealed from microscopy and there is a high probability that positrons may get trapped at these interfaces. The trapping of positrons at the incoherent interface of α-precipitate (i.e. Cr precipitate) in high Cr content Ni alloy during thermal ageing has been earlier reported by Druzhkov et al. [38] using Angular correlation of annihilation radiation (ACAR) measurements. The τ_2 values indicate that the size of open-volume defects at these interfaces is in the range of size of vacancy clusters. The decrease in τ_2 can be attributed to an increase in the coherency at the interface as precipitates grow in size with time. During DP reaction, the precipitates grow in a manner to reduce incoherency at the interface which shows that open-volume size would tend to decrease when precipitates grow due to the tendency to reduce lattice mismatch [39, 40]. Therefore, we may infer that vacancy-like defects/vacancy-solute complexes and precipitate's interface are the predominant positron trapping sites in the studied alloy under thermal ageing. The former predominates during the initial stages of phase separation whilst later contributes towards positron trapping with subsequent ageing.

In order to investigate the characteristics of the defects/positron trapping sites, the momentum distribution of annihilation electrons around the trapping site is measured using CDB which is sensitive to the chemical surrounding of the defects. The CDB curves for aged samples plotted as the ratio with

respect to pure Ni are shown in Fig. 7. The ratio curve for pure Cr is shown as a reference. The ratio curves for all the aged alloys show the characteristic feature of Cr indicating that positrons are trapped at sites decorated with Cr atoms. However, the amplitude of the curves indicates that only 50% of the neighboring atoms at the trapping sites are of Cr. There is no significant change in the ratio curves for all the aged alloys except the alloy aged for 24 h at 800 °C. The ratio curve for this sample shifts more towards Cr reference indicating an enhancement in the number of Cr atoms surrounding the trapping site. In addition, there is a significant increase in the low momentum region for this sample. The enhancement in the low momentum region signifies that more positrons are trapped in vacancies. At 24 h ageing at 800 °C, nearly complete phase transformation, i.e. Cr segregation has taken place; therefore, vacancies with Cr atoms surrounding would be primarily located within the Cr precipitates. Thus, we may conclude that for the highest ageing treatment studied (24 h at 800 °C) positrons are trapped in the Cr precipitates. It is worth mentioning here that Cr has a lower positron affinity than Ni and therefore, positrons will trap in Cr precipitates when defects are present. This shows that vacancy-like defects are evolved in Cr precipitates only at longer ageing. On the other hand, for all other aged samples, positrons are trapped at sites with nearly 50% surrounding Cr atoms. Since the studied alloy is a solid-solution of the nearly equal atomic composition of Ni and Cr, the thermally generated vacancies would not be specific to either Ni or Cr. Also, the annihilation from the vacancy-solute complex with only a few Cr atoms would not be reflected as a remarkable feature in the momentum distribution curve. Similar characteristics of momentum distribution have been suggested for vacancy-solute complexes in a number of Fe-based alloys where momentum distribution curves do not show remarkable features due to only a fewer number of solute atoms in the vacancy-solute complex [41]. In the same way, the interface of Cr precipitate and matrix is likely to have a nearly equal contribution from Ni and Cr. Thus, in the present alloy, it is very difficult to segregate the contributions of vacancies and the precipitate's interface at different stages of precipitation due to nearly similar characteristics of the momentum distribution of the 2. However, based on PL measurements in conjunction with microscopy results, we may state that vacancy
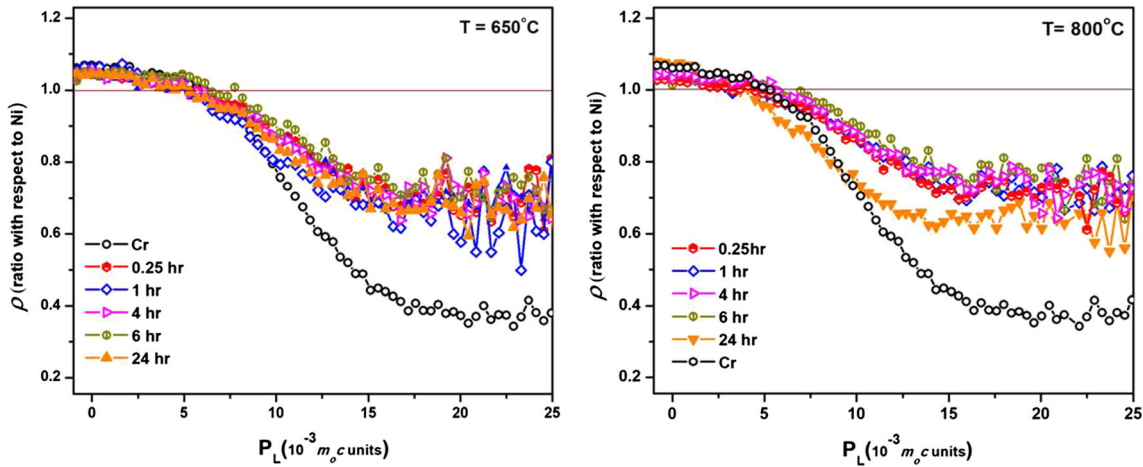
Figure 7 Momentum distribution curve (obtained from CDB) for Ni–Cr alloy aged at 650 °C and 800 °C. The curves are plotted as ratio with respect to pure Ni.

cluster/vacancy-solute complex are predominant positron trapping sites during the initial stage of phase separation whilst precipitate's interfaces predominate during the later stage of phase segregation. The results also reveal that there is a possibility of the presence of defects within Cr precipitates once the complete phase transformation has taken place. For the studied alloy, we must admit that due to low sensitivity of positron towards Cr precipitate in Ni matrix lead to reduced positron response (i.e. trapping) in comparison to the case of Cu precipitates in Fe–Cu alloy as studied by He et al. [22] where positrons are predominantly confined in Cu precipitates.

The positron annihilation in the studied alloy indicates that observed defects are not effective positron traps. Only less than 50% of the positrons are annihilating from the trapped state in the alloy. Even at 24 h ageing (at 800 °C) when ∼ 100% phase transformation is achieved and precipitates occupy a large fraction of the grain volume, saturation trapping is not observed. This indicates that the positron trapping rate for defects in the alloy is small. Based on our results and observations, we have estimated the positron specific trapping rate for the interfaces in order to estimate the number density of precipitates in the alloy. In earlier reports, the growth behaviour of precipitates has shown an increase in interlamellar distance (distance between the precipitates) during ageing due to coalescence [18]. Due to an increase in interlamellar distance and thereby reduction in the number density of precipitates and hence the interfaces, saturation trapping is not achieved even at the longest ageing period studied. As mentioned

previously that positron trapping at precipitate's interfaces increases with ageing, we may estimate positron specific trapping coefficient (μ_d) for interfaces. The positron trapping at the interfaces is limited by diffusion of positron to these interfaces [24]. Assuming the trapping at the surface of a precipitate, μ_d can be expressed as [20, 42] $\mu_d = 4\pi r D_+$, where r is the effective radius of the positron trapping site and D_+ is the positron diffusion coefficient. The trapping at the interface is expected when the diffusion length of the positron is of the order of the mean distance between the precipitates. We have independently evaluated interlamellar distance from microscopic measurements, and it varies from 200 to 450 nm at 2 h ageing for different temperatures [18]. Assuming positron diffusion length (L_+) to be ∼ 200 nm (for ageing at 800 °C) and τ_b ∼ 115 ps, the calculated D_+ = 2.66 cm^2 s^{-1} using the following relation: $L_+ = \sqrt{D_+ \tau_b}$. As for r, the size of lattice misfits (open-volume defect) at the interface can be considered to be of the order of a few Å. Considering $r = 4$ Å, the estimated μ_d is ∼ 1.33×10^{-6} cm^3 s^{-1} which is of the order estimated for large voids [31]. We may assume that at 800 °C ageing for 6 h, interfaces are the predominant trapping sites as precipitates have occupied a substantial volume of the grains. The number density of precipitates at 6 h ageing can be approximated as ∼ 10^{15} cm^{-3}. It is to be noted that the estimated number density is just an approximation as positron is not trapped within the precipitates. The number density of precipitates formed via DP is generally difficult to estimate as precipitation is not homogeneously distributed in the matrix. A rigorous

scanning and statistics are required to obtain the exact estimation. In this regard, the estimated number density from positron annihilation is a good approximation to quantify DP transformations.

Conclusions

We have investigated the evolution of defects during thermal treatment in high Cr content Ni–Cr (42 wt% Cr) alloy using positron annihilation spectroscopy complemented with microscopic techniques. Thermal treatment at 650 °C and 800 °C resulted in phase transformation of the matrix through precipitation of Cr via discontinuous precipitation reaction. The kinetics of precipitation is seen to be faster at 800 °C than 650 °C wherein, in the former case precipitates occupy a large volume of the grains within 24 h of ageing. The defects evolved during the thermal treatment of the alloy are primarily thermal vacancies, interface between precipitate and matrix and vacancy-like defects. The results show that thermally generated vacancies during solutionization treatment are stabilized in gamma-quenched sample by forming the vacancy-Cr solute complexes, which acts as nucleation sites for Cr aggregation. In the aged alloys, vacancy-defect (vacancy clusters and/or vacancy-Cr solute complex) and the interface between Cr precipitate and matrix are the trapping sites for positrons. During the initial stage of ageing, positrons are trapped mainly at vacancy-like defects whilst precipitate's interfaces predominate with subsequent ageing. Coincidence Doppler broadening results indicate that vacancy defects not specific to Ni or Cr atoms and surround the trapping site in nearly equal proportions, thereby, giving a similar response as due to positron trapping at the precipitate's interface. Therefore, unambiguous identification of defect type at each stage of precipitation is difficult in the present alloy. Considering positron trapping at the surface of precipitates, we calculated positron specific trapping coefficient for the interfaces and estimated the number density of precipitates. The number density obtained from the positron annihilation technique can be a good approximation to quantify and probe DP transformations in alloys.

Compliance with ethical standards

Conflict of interest The authors declare that they have no conflict of interest.

References

[1] Danoix F, Bémont E, Maugis P (2006) Atom probe tomography i: early stage of precipitation of NbC and NbN in Ferretic Steel. Adv Eng Mater 8:1202

[2] Gladman T (1999) Precipitation hardening in metals. Mater Sci Technol 15(1):30–36

[3] Gupta AK, Lloyd DJ, Court SA (2001) Precipitation hardening in Al–Mg–Si alloys with and withoutexcess Si. Mater Sci Eng A 316:11–18

[4] Correia JB, Davies HA, Sellars CM (1997) Strengthening in rapidly solidified age hardened Cu-Cr and Cu-Cr-Zr alloys. Acta Mater 45(1):177–190

[5] Jiao ZB, Luan JH, Miller MK, Yu CY, Liu CT (2016) Group precipitation and age hardening of nanostructured Fe-based alloys with ultra-high strengths. Sci Rep 6:21364–21377

[6] Reed RC (2006) The superalloys: fundamentals and applications edited. Cambridge university press, New York

[7] Epler M (2004) ASM Handbook. In: G.F. Vander Voort (ed) Metallography and Microstructures, vol 9, p 134–139

[8] Macchi C, Tolley A, Giovachini R, Polmear IJ, Somoza A (2015) Influence of a microalloying addition of Ag on the precipitation kinetics of an Al–Cu–Mg alloy with high Mg: Cu ratio. Acta Mater 98:275–287

[9] Somoza A, Petkov MP, Lynn KG, Dupasquier A (2002) Stability of vacancies during solute clustering in Al-Cu-based alloys. Phys Rev B 65:094107–094113

[10] Soisson F, Jourdan T (2016) Radiation-accelerated precipitation in Fe–Cr alloys. Acta Mater 103:870–881

[11] Yan Z, Shi S, Li Y, Chen J, Maqbool S (2020) Vacancy and interstitial atom evolution with the separation of the nanoscale phase in Fe–Cr alloys: phase-field simulations. Phys Chem Chem Phys 22(2020):3611–3619

[12] Nash P (1986) The Cr–Ni system. Bull Alloy Phase Diagr 7:466–476

[13] Pyczak F, Devrient B, Neuner FC, Mughrabi H (2005) The influence of different alloying elements on the development of the γ/γ microstructure of nickel-base superalloys during high-temperature annealing and deformation. Acta Mater 53:3879–3891

[14] Zheng L, Xiao C, Zhang G, Han B, Tang D (2012) J Alloy Comp 52:176

[15] MacKay RA, Gabb TP, Garg A, Rogers RB, Nathal MV (2012) Influence of composition on microstructural parameters of single crystal nickel-based superalloys. Mater Charact 70:83–100

[16] Ming H, Liu X, Yan H, Zhang Z, Wang J, Gao L, Lai J (2019) En-Hou Han, Understanding the microstructure evolution of Ni-based superalloy within two different fretting wear regimes in high temperature high pressure water. Scr Mater 170:111–115

[17] "Nickel–Chromium (Ni-Cr) Phase Diagram," (2006) www.calphad.com

[18] Keskar N, Pattanaik AK, Mani Krishna KV, Srivastava D, Dey GK (2017) Kinetics and grain boundary selectivity of discontinuous precipitation in Ni-Cr alloy. Met Mater Trans A 48(6):3096–3106

[19] Manna I, Pabi SK, Gust W (2001) Discontinuous reactions in solids. Int Mater Rev 46(2):53–91

[20] Inoue K, Nagai Y, Tang Z, Toyama T, Hosoda Y, Tsuto A, Hasegawa M (2011) Time evolution of positron affinity trapping at embedded nanoparticles by age-momentum correlation. Phys Rev B 83:115459–115464

[21] Toyama T, Tang Z, Inoue K, Chiba T, Ohkubo T, Hono K, Nagai Y, Hasegawa M (2012) Size estimation of Cu embedded nanoprecipitates in Fe by using affinitively trapped positrons. Phys Rev B 86:104106–104113

[22] He SM, van Dijk NH, Schut H, Peekstok ER, van der Zwaag S (2010) Thermally activated precipitation at deformation-induced defects in Fe–Cu and Fe-Cu-B-N alloys studied by positron annihilation spectroscopy. Phys Rev B 81:094103–094113

[23] Nagai Y, Hasegawa M, Tang Z, Hempel A, Yubuta K, Shimamura T, Kawazoe Y, Kawai A, Kano F (2000) Positron confinement in ultrafine embedded particles: quantum-dot-like state in an Fe–Cu alloy. Phys Rev B 61(10):6574–6579

[24] Čížek J, Melikhova O, Procházka I, Kuriplach J, Stulíková I, Vostrý P, Faltus J (2005) Annealing process in quenched Al-Sn alloys: a positron annihilation study. Phys Rev B 71:0641106–0641119

[25] Staab TEM, Krause-Rehberg R, Kiebak B (1999) Positron annihilation in fine grained materials and fine powders: an application to the sintering of metal powders. J Mater Sci 34:3833. https://doi.org/10.1023/A:1004666003732

[26] Kirkegaard P, Olsen JV, Eldrup MM, Pedersen NJ (2009) PALSfit. Roskilde: Danmarks Tekniske Universitet, Risø National laboratoriet for BæredygtigEnergi. (Denmark. Forskningscenter Risoe. Risoe-R; No. 1652(EN))

[27] Sharma SK, Sudarshan K, Maheshwari P, Dutta D, Pujari PK, Shah CP, Kumar M, Bajaj P (2011) Direct evidence of Cd vacancies in CdSe nanoparticles: positron annihilation studies. Eur Phys J B 82:335–340

[28] Campillo Robles JM, Ogando E, Plazaola F (2007) Positron lifetime calculation for the elements of periodic table. J Phys Condens Matter 19:176222

[29] Kuramoto E, Tsutsumi T, Ueno K, Ohmura M, Kamimura Y (1999) Positron lifetime calculations on vacancy clusters and dislocations in Ni and Fe. Comput Mater Sci 14:28–35

[30] Lawrence SK, Yagodzinskyy Y, Hanninen H, Korhonen E, Tuomisto F, Harris ZD, Somerday BP (2017) Effects of grain size and deformation temperature on hydrogen-enhanced vacancy formation in Ni alloys. Acta Mater 128:218–226

[31] Krause-Rehberg R, Leipner HS (eds) (1999) Positron annihilation in semiconductors. Springer, Berlin

[32] Puska MJ, Corbel C, Nieminen RM (1999) Positron trapping in semiconductors. Phys Rev B 41:9980–9994

[33] Korhonen T, Puska MJ, Nieminen RM (1995) Vacancy formation energy for fcc and bcc transition elements. Phys Rev B 51:9526–9533

[34] Unzueta I, Sánchez-Alarcos V, Recarte V, Pérez-Landazábal JI, Zabala N, García JA, Plazaola F (2019) Identification of a Ni-vacancy defect in Ni-Mn- Z (Z = Ga, Sn, In): an experimental and DFT positron-annihilation study. Phys Rev B 99:064108–064120

[35] Puska MJ, Niemenn RM (1994) Theory of positron in solids and on solid surfaces. Rev Mod Phys 66:841–900

[36] Dupasquier A, Mills AP (eds) (1995) Positron spectroscopy of solids. IOS press, Amsterdam

[37] Mao Z, Booth-Morrison C, Sudbrack CK, Martin G, Seidman DN (2012) Kinetic pathways for phase separation: an atomic scale study in Ni-Al-Cr alloys. Acta Mater 60:1871–1888

[38] Druzhkov AP, Kolotushkin VP, Arbuzov VL, Danilov SE, Perminov DA (2006) Structural and phase states and irradiation-induced defects in Ni–Cr Alloys. Phys Met Metallogr 101:369–378

[39] Fournelle RA, Clark JB (1972) The genesis of the cellular precipitation reaction. Met Trans 3:2757–2768

[40] Findik F (1998) Discontinuous (cellular) precipitation. J Mater Sci Lett 17:79–83

[41] Nagai Y, Takadate K, Tang Z, Ohkubo H, Sunaga H, Takizawa H, Hasegawa M (2003) Positron annihilation study of vacancy-solute complex evolution in Fe-based alloys. Phys Rev B 67:224202–224208

[42] Brandt W, Paulin R (1972) Positron diffusion in solids. Phys Rev B 5:2430–2435